Electronic Supplementary Material (ESI) for ChemComm.

Electronic Supplementary Information (ESI)

A drastic change in the superhydrophilic crystal porosities of metallosupramolecular structures via a slight change in pH

Sireenart Surinwong, Nobuto Yoshinari, Tatsuhiro Kojima and Takumi Konno*

Department of Chemistry, Graduate School of Science, Osaka University, Toyonaka, Osaka 560-0043 (Japan)
konno@chem.sci.osaka-u.ac.jp

Preparation of complexes

(a) Preparation of $[\mathrm{Zn(H_2O)_4}\{\mathrm{Co_2Au_3}(\text{D-Hpen-}N,S)(\text{D-pen-}N,S)_5\}]$ (1)

To a purple solution containing $\mathrm{Na_3[Co_2Au_3}(\text{D-pen-}N,S)_6]\cdot 13\mathrm{H_2O}$ (50 mg, 0.030 mmol) in a sodium acetate buffer solution (2.5 mL, pH 5.0, $[\mathrm{OAc^-}]$ = 0.7 M), a colourless solution of $\mathrm{Zn(OAc)_2\cdot 2H_2O}$ (10 mg, 0.045 mmol) in an aqueous NaOAc buffer solution (2.5 mL, pH 5.0, $[\mathrm{OAc^-}]$ = 0.7 M) was added. The mixture was stirred at room temperature for 5 min, yielding a clear dark-purple solution. After the reaction solution was allowed to stand at room temperature for 1 day, purple square block crystals (**1**) appeared, which were collected by filtration. Yield: 32 mg (58%). Anal. Calcd for $[\mathrm{Zn(H_2O)_4}\{\mathrm{Co_2Au_3}(\text{D-Hpen-}N,S)(\text{D-pen-}N,S)_5\}]\cdot 5\mathrm{H_2O}$ = $\mathrm{C_{30}H_{73}N_6S_6O_{21}Co_2Au_3Zn}$: C, 19.79; H, 4.04; N, 4.62%. Found: C, 19.75; H, 3.95; N, 4.60%. IR ($\mathrm{cm^{-1}}$, KBr disk): 1609 ($\nu_{\mathrm{COO^-}}$), 1717 $(\nu_{\mathrm{COOH}})^{\mathrm{sh}}$. The ^{23}Na NMR spectrum of **1** in $\mathrm{DCl/D_2O}$ showed no signals from $\mathrm{Na^+}$.

(b) Preparation of $\mathrm{Na_9[Zn(OAc)_2}\{\mathrm{Co_2Au_3}(\text{D-pen-}N,S)_6\}_2][\mathrm{Co_2Au_3}(\text{D-pen-}N,S)_6]$ (2)

To a purple solution containing $\mathrm{Na_3[Co_2Au_3}(\text{D-pen-}N,S)_6]\cdot 13\mathrm{H_2O}$ (50 mg, 0.030 mmol) in a sodium acetate buffer solution (2.5 mL, pH 5.5, $[\mathrm{OAc^-}]$ = 0.9 M), a colourless solution of $\mathrm{Zn(OAc)_2\cdot 2H_2O}$ (10 mg, 0.045 mmol) in an aqueous NaOAc buffer solution (2.5 mL, pH 5.5, $[\mathrm{OAc^-}]$ = 0.9 M) was added. The mixture was stirred at room temperature for 5 min, which gave a clear, dark-purple solution. After the reaction solution was allowed to stand at room temperature for 2 weeks, purple hexagonal block crystals (**2**) appeared, which were collected by filtration. Yield: 14 mg (23%). Anal. Calcd for $\mathrm{Na_9[Zn(OAc)_2}\{\mathrm{Co_2Au_3}(\text{D-pen-}N,S)_6\}_2][\mathrm{Co_2Au_3}(\text{D-pen-}N,S)_6]\cdot 36\mathrm{H_2O}$ = $\mathrm{C_{94}H_{240}N_{18}S_{18}O_{76}Co_6Au_9Na_9Zn}$: C, 19.42; H, 4.16; N, 4.34%. Found: C, 19.44; H, 4.11; N, 4.18%. IR ($\mathrm{cm^{-1}}$, KBr disk): 1611 ($\nu_{\mathrm{COO^-}}$).

The ^{23}Na NMR spectrum of **2** in $\mathrm{D_2O}$ showed an intense signal from hydrated $\mathrm{Na^+}$ ions at δ 0.0 ppm (ppm from NaCl). The number of $\mathrm{Na^+}$ ions per formula unit of **2** was evaluated to be 8.7 from integration of the ^{23}Na signal, which is comtatible with the ideal value of 9 for the chemical formula of **2**.

(c) Controlled experiment using pH 5.0 solution containing amounts of $\mathrm{Na^+}$ and $\mathrm{OAc^-}$ ions equal to those of 2

A 0.5 M aqueous HCl solution was added to a sodium acetate buffer solution (pH 5.5, $[\mathrm{OAc^-}]$ = 0.9 M) until a pH of 5.0 was achieved. The solution was used as a solvent for an analogous experiment for the preparation of **2** (experiment (b)). Purple square block crystals of **1**, which were characterized by powder X-ray diffraction analysis (Fig. S13), were obtained after 1 day. Yield: 11 mg (21%).

Similar experiments using pH 4.0 and pH 4.5 also gave **1**.

(d) Interconversion between 1 and 2.

To a dark purple solution containing 12 mg (6.6 μmol) of **1** in 10 mL of 0.5 M HCl aqueous solution was added a 0.5 M NaOH aqueous solution until the solution became pH 7. The solution was evaporated to dryness with a rotary evaporator, and then, a sodium acetate buffer solution (5 mL, pH 5.5, [OAc$^-$] = 0.9 M) was added to it. When the dark purple solution was allowed to stand at room temperature for 3 weeks, purple hexagonal block crystals (**2**) appeared, which were collected by filtration and washed with acetone. Yield: 4 mg (31%). The powder X-ray diffraction (PXRD) pattern of the purple hexagonal block crystals thus obtained was essentially similar to that of **2**.

The reverse conversion from **2** to **1** was also achieved by the following procedure: a 15 mg sample of **2** (2.6 μmol) was dissolved in a sodium acetate buffer solution (5 mL, pH 5.0, [OAc$^-$] = 0.9 M), which gave a dark purple solution. When the dark purple solution was allowed to stand at room temperature for 3 days, purple square block crystals (**1**) appeared, which were collected by filtration and washed with acetone. Yield: 3 mg (64%). The PXRD pattern of the purple square block crystals thus obtained was the same as that of **1**.

Physical measurements

Diffuse-reflectance spectra were recorded with a JASCO V-570 UV/VIS/NIR spectrometer at room temperature. The circular dichroism (CD) spectra in the solid state were performed on a JASCO J-820 spectropolarimeter at room temperature. The IR spectra were recorded with a JASCO FT/IR-4100 infrared spectrometer using KBr disks at room temperature. Elemental analyses (C, H, N) were performed at Osaka University using a Yanaco CHN Corder MT-5. The X-ray fluorescence analyses were conducted using a SHIMADZU Rayny EDX-720 spectrometer. ^{1}H NMR spectra were recorded with a JEOL ECAMX-500SP spectrometer in D_2O with sodium 4,4-dimethyl-4-silapentane-1-sulfonate (DSS) used as an internal reference. The ^{23}Na NMR spectra were recorded with a JEOL JNM-ECS400 spectrometer in D_2O with sodium chloride as an external reference. All measurements were performed at probe temperature. The sorption isotherms of N_2 and CO_2 were measured with a BELSORP-mini II volumetric adsorption instrument. N_2 and CO_2 gases of high purity (99.9999%) were used. The sorption isotherms for H_2O, EtOH, and acetone were obtained with a BELSORP-max volumetric adsorption instrument. The obtained crystals were heated at 120°C for 2 h under a reduced pressure before gas sorption measurements. High-quality powder X-ray diffractions were recorded at room temperature, in transmission mode [synchrotron radiation λ = 0.999139(2) Å; 0° ≤ 2θ ≤ 78°; step width = 0.005°; data collection time = 1 min] on a diffractometer equipped with a MYTHEN microstrip X-ray detector (Dectris Ltd.) at the SPring-8 BL02B2 beamline. The crystals were loaded into glass capillary tubes (diameter = 0.3 mm), and the samples were rotated during the measurements. The diffraction data were collected with a large Debye-Scherrer camera. The powder simulation patterns were generated from the single-crystal X-ray structures using the Mercury 3.8 software.

X-ray crystal structural determinations

Single-crystal X-ray diffraction data for **1** were recorded on a Rigaku Mercury 2 CCD detector with synchrotron radiation (λ = 0.6997 Å) at the BL02B1 beamline in SPring-8 with the approval of the Japan Synchrotron Radiation Research Institute (JASRI). The intensity data were collected by the ω-scan technique and were processed with the Rapid Auto software program. The structure of **1** was determined by direct methods using the SHELXS-2014 program. Structural refinements were carried out using the full-matrix least-squares method (SHELXL-2014). All calculations were performed using the WinGX software package. All non-hydrogen atoms except for disordered carboxylate part were refined anisotropically. Hydrogen atoms were included in the calculated positions except for those belonging to water molecules. A restraint (ISOR) was applied for an isolated solvated water.

Single-crystal X-ray diffraction data for **2** were recorded on an ADSC Q210 CCD area detector with synchrotron radiation (λ = 0.7000 Å) at the 2D beamline in Pohang Accelerator Laboratory (PAL). The intensity data were collected by the ω-scan technique, and the diffraction images were processed using the HKL3000 program. Absorption correction was also performed using the PLATON program. The structure of **2** was solved by direct methods using SHELXS-2014. First, the structural refinements were carried out using full-matrix least-squares (SHELXL-2014) for the original intensity data. All calculations were performed using the WinGX software package. The crystal structure possesses a large void space (29,406 A^3, calcd by PLATON) in a one dimensional structure composed of Na^+ cations, $[Co_2Au_3(\text{D-pen-}N,S)_6]^{3-}$ anions and $\{Zn(OAc)_2\}$ moieties. The void space is assumed to be filled with the solvated water molecules and Na^+ ions based on the elemental, fluorescence X-ray, ^{23}Na NMR, and thermogravimetric analyses, although all molecules were not modeled well. The estimated numbers of the solvated water and Na^+ ions per a formula unit from volume calculation are about 116 and 7, respectively. Furthermore, the PLATON SQUEEZE reported 1281 electrons in the void space per a formula unit, corresponding to 120 water molecules and 7 Na^+ ions, which is close to the estimation from volume calculation. In addition to the other chemical analysis, these results support that the void space is fully occupied by the solvated water molecules and Na^+ ions. Therefore, the PLATON SQUEEZE was applied for the subtraction of the contribution of water and Na^+ ions from observed intensity to refine the main framework. With using intensity data corrected by SQUEEZE, the main framework was refined again by the full-matrix least-squares with SHELXL-2014. All non-hydrogen atoms were refined anisotropically. Hydrogen atoms were included in the calculated positions. Several restraints (SIMU, DELU and DFIX) were applied to model the carboxylate group and the acetate.

Table S1. Crystallographic data for **1** and **2**.

	1	**2**
Formula	$C_{30}H_{55}Au_3Co_2N_6O_{18}S_6Zn$	$C_{94}H_{168}Au_9Co_6N_{18}Na_2O_{50}S_{18}Zn$
Colour, form	Purple, square block	Purple, hexagonal block
Mw	1754.29	5165.16
Crystal system	Orthorhombic	Hexagonal
Space group	$I222$	$P6_122$
a/ Å	10.307(3)	44.24850(10)
b/ Å	18.544(5)	44.24850(10)
c/ Å	27.144(7)	28.44460(10)
α((°)	90	90
β (°)	90	90
γ (°)	90	120
V/ Å^3	5188(2)	48231.1(3)
Z	4	6
T/ K	100(2)	100(2)
F(000)	3352	14826
μ(Mo Kα)/ mm^{-1}	9.140	4.286
Crystal size /mm^3	0.10×0.06×0.06	0.18×0.15×0.11
Limiting indices	$-13 \le h \le 12$, $-24 \le k \le 23$, $-35 \le l \le 34$	$-64 \le h \le 56$, $-56 \le k \le 60$, $-37 \le l \le 37$
$2\theta_{max}$(°)	54.08	66.79
$R1$ ($I>2\sigma(I)$)[a)]	0.0383	0.0627
w$R2$ (all data) [b)]	0.0818	0.1702
GOF	1.012	1.056

a) $R1 = \Sigma||F_o|-|F_c||/\Sigma|F_o|$.

b) $wR2 = [\Sigma(w(F_o^2-F_c^2)^2) / \Sigma w(F_o^2)^2]^{1/2}$.

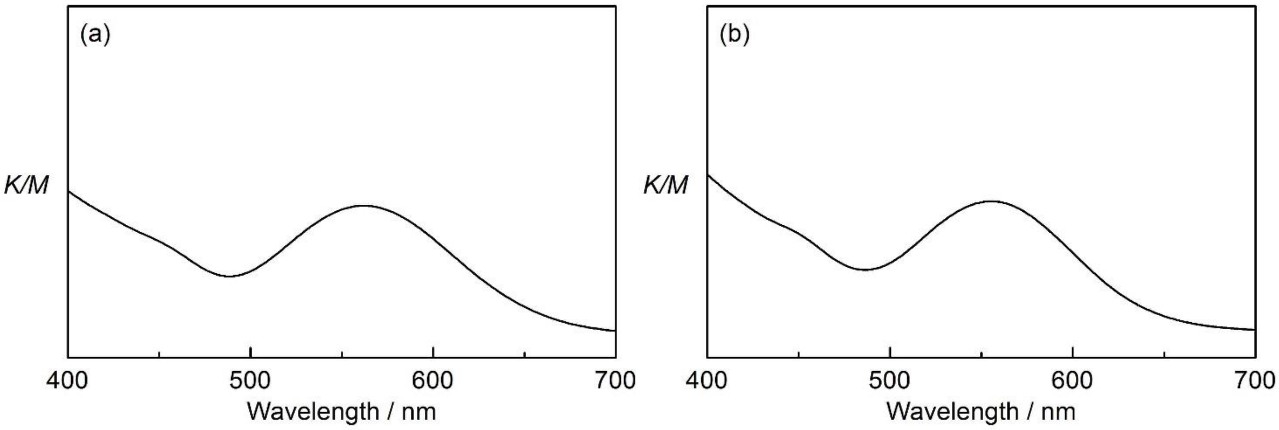

Fig. S1 Diffuse reflection spectra of (a) **1** and (b) **2**.

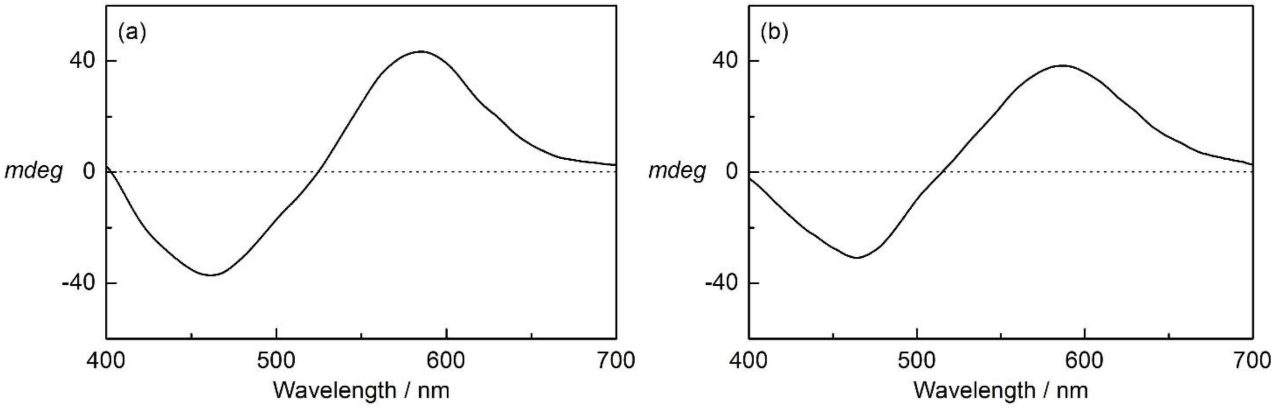

Fig. S2 Solid-state CD spectra of (a) **1** and (b) **2**.

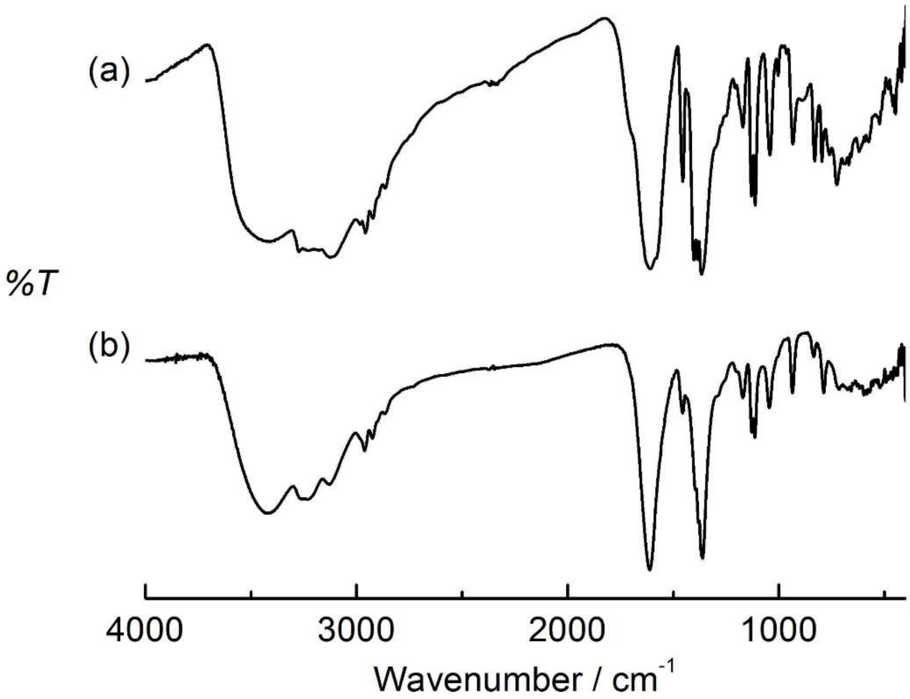

Fig. S3 IR spectra of (a) **1** and (b) **2**.

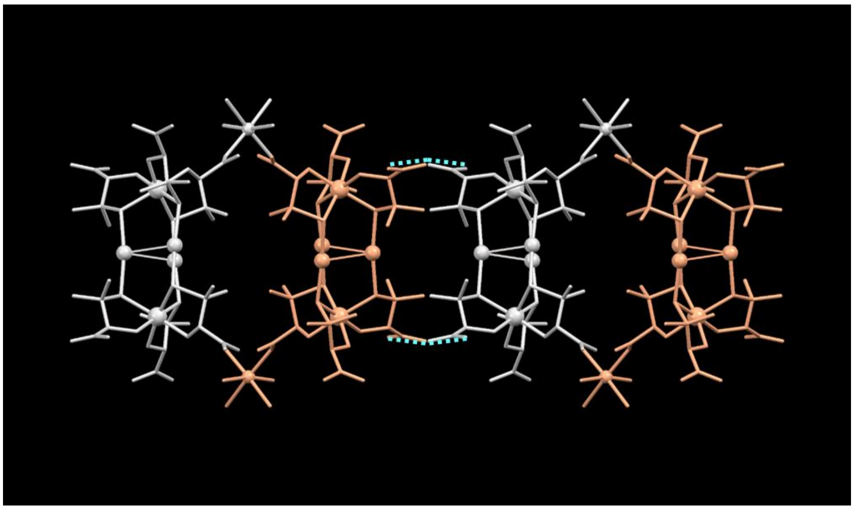

Fig. S4 Top view of the two double helices (orange and white) connected by intermolecular hydrogen-bonding interactions in **1**. Dashed lines indicate hydrogen bonds.

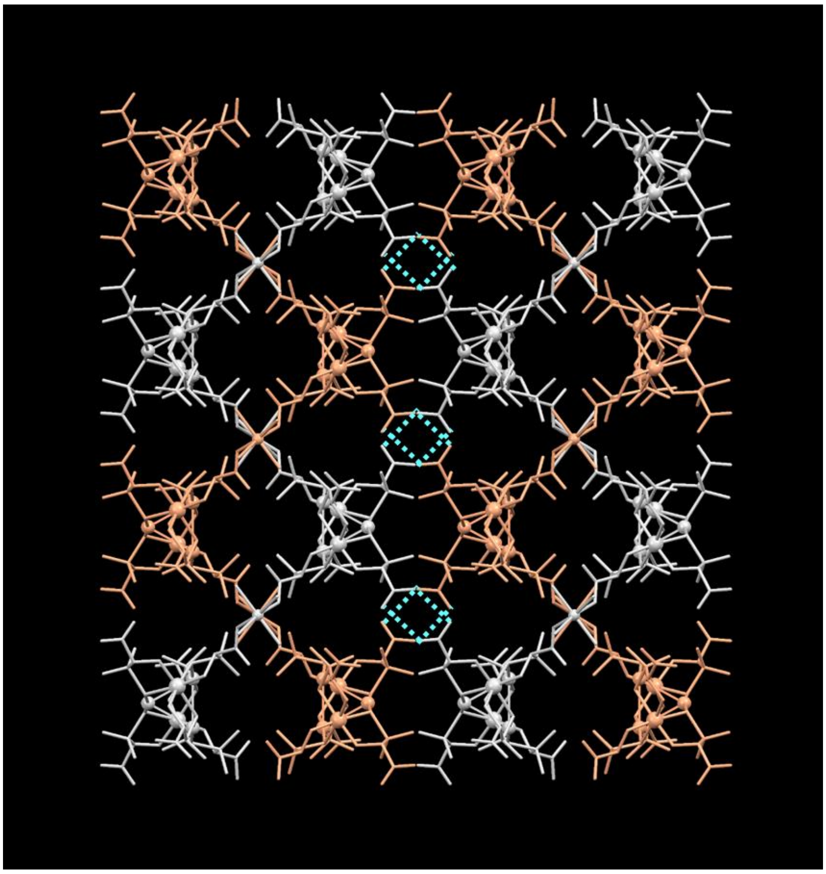

Fig. S5 Side view of the two double helices (orange and white) connected by intermolecular hydrogen-bonding interactions in **1.** Dashed lines indicate hydrogen bonds.

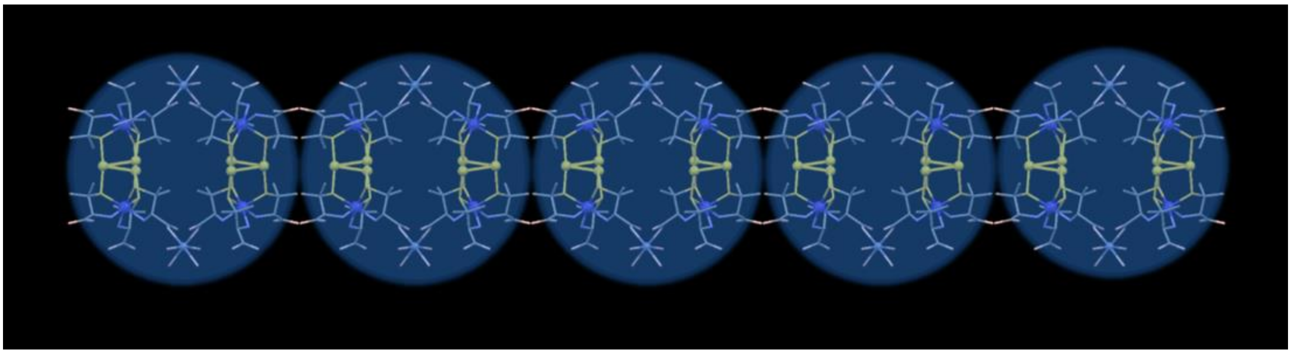

Fig. S6 A 2D sheet-like structure in **1**. Blue circles indicate each 1D coordination double helix.

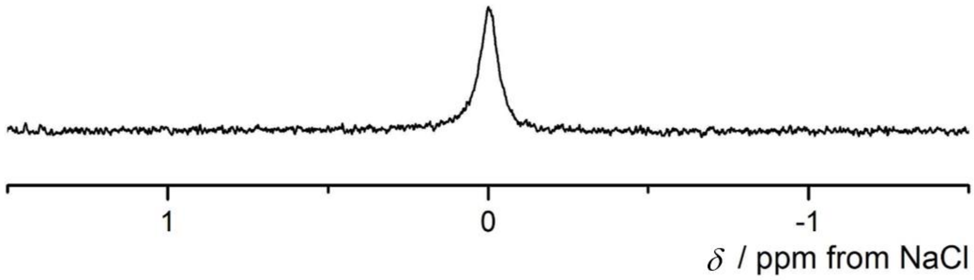

Fig. S7 ^{23}Na NMR spectrum of **2** in D_2O.

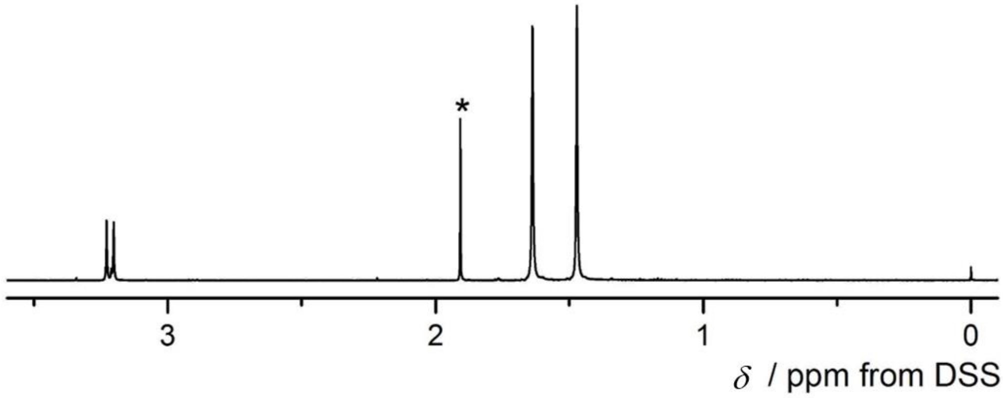

Fig. S8 ^{1}H NMR spectrum of **2** in D_2O. (*) denotes a signal from acetate.

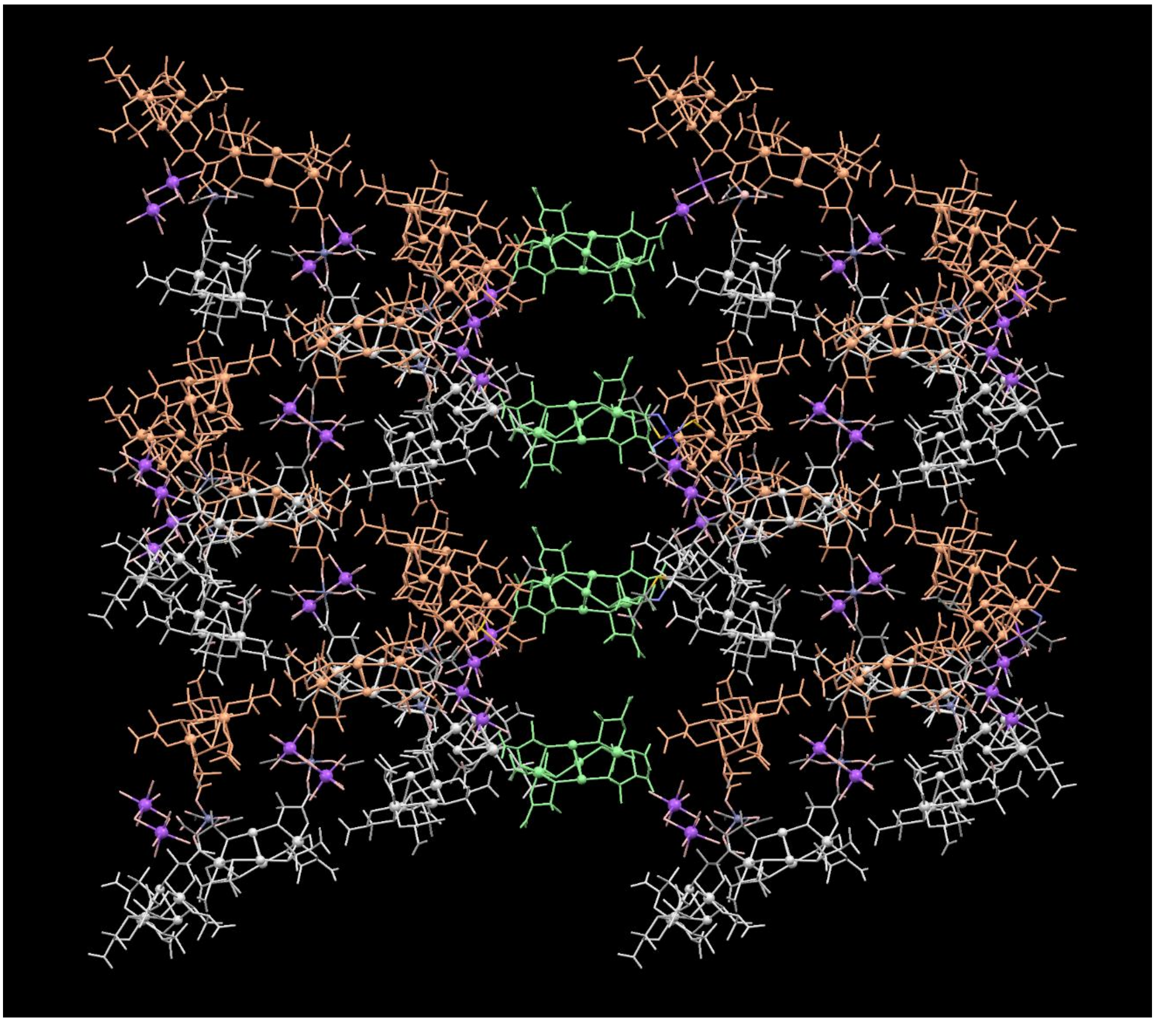

Fig. S9 Two double helices (orange and white) connected by $[Co_2Au_3(\text{D-pen-}N,S)_6]^{3-}$ anions (green) in **2**.

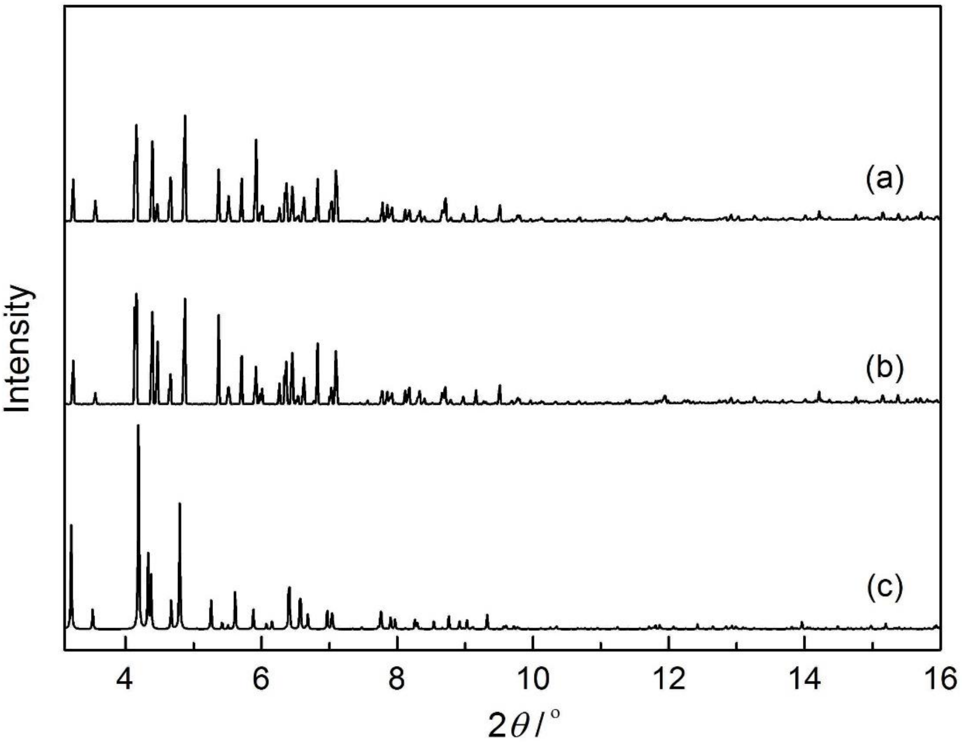

Fig. S10 Experimental PXRD patterns (a) after and (b) before heating at 120°C, and (c) the simulated PXRD pattern of **2**.

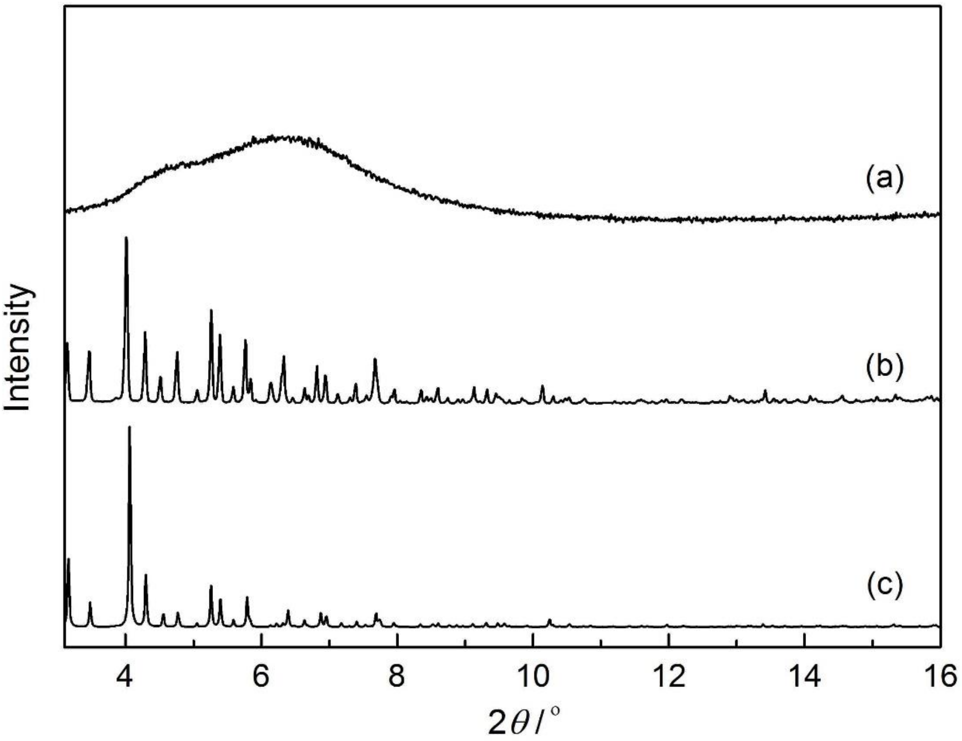

Fig. S11 Experimental PXRD patterns (a) after and (b) before heating at 120°C, and (c) the simulated PXRD pattern of **3**.

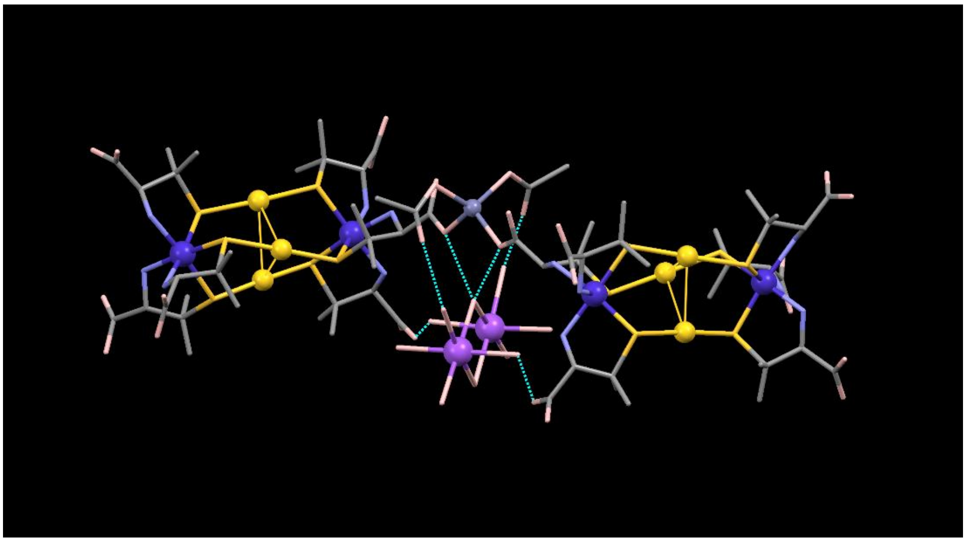

Fig. S12 The multiple hydrogen bonds between $[Na_2(H_2O)_{10}]^{2+}$ cations and $[Zn(OAc)_2\{Co_2Au_3(\text{D-pen-}N,S)_6\}_2]^{4-}$ anions observed in **2**. Color codes: Zn, dark grey; Na, red purple; Co, deep blue; Au, gold; S, yellow; O, pink; N, blue; C, grey. Dashed lines indicate hydrogen bonds.

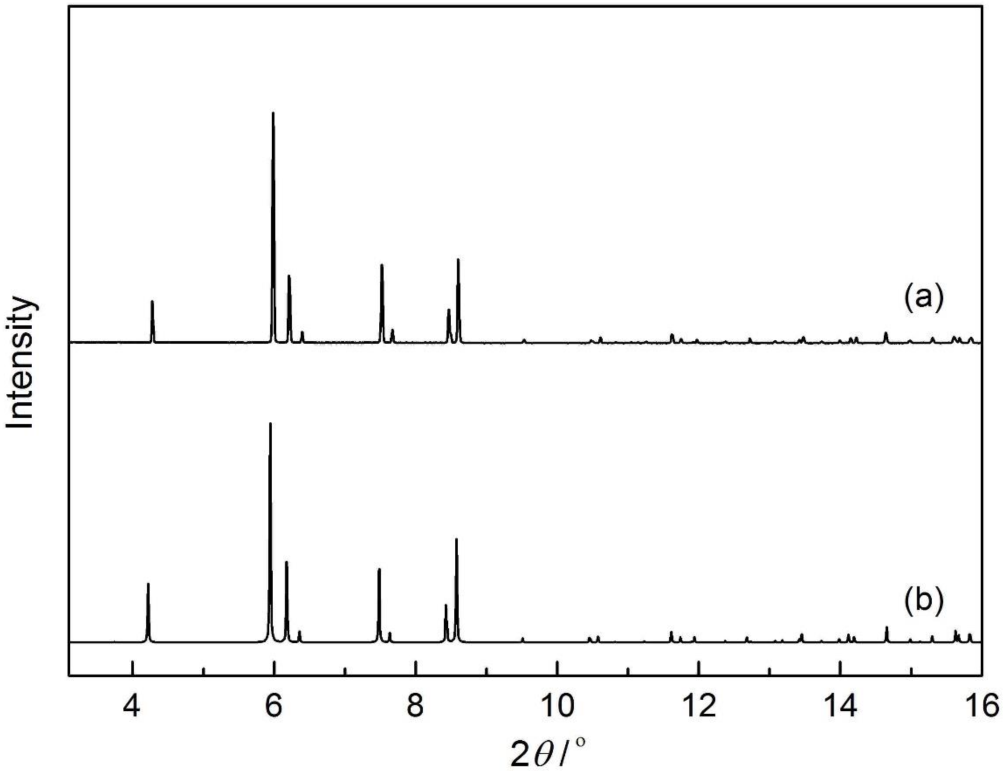

Fig. S13 (a) Experimental PXRD pattern of **1** obtained from the controlled experiment and (b) simulated PXRD pattern of **1**.

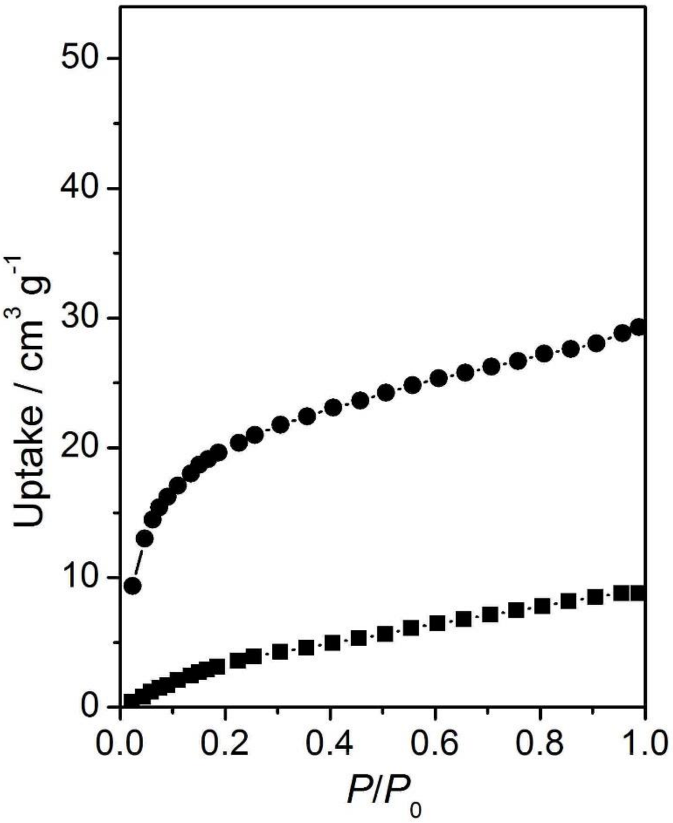

Fig. S14 Comparison of CO_2 adsorption isotherms at 195 K for **1** (–■–) and **2** (–●–).

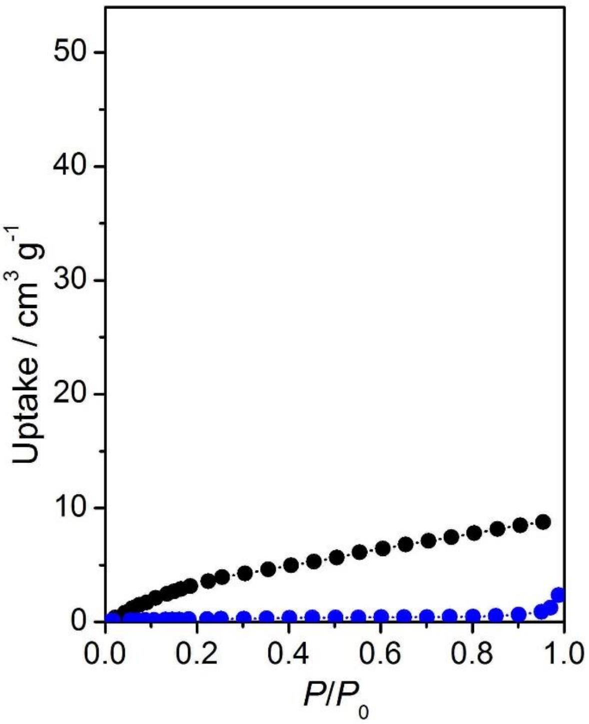

Fig. S15 Comparison of CO_2 at 195 K (black) and N_2 at 77 K (blue) adsorption isotherms for **1**.

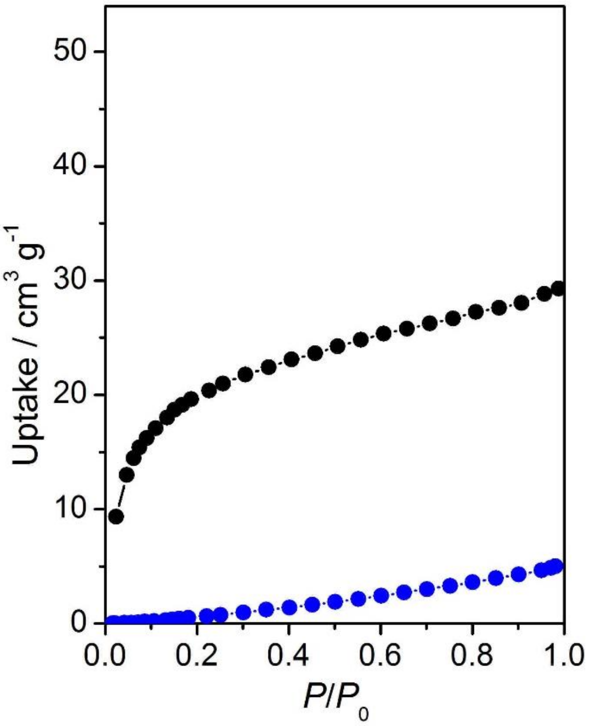

Fig. S16 Comparison of CO_2 at 195 K (black) and N_2 at 77 K (blue) adsorption isotherms for **2**.

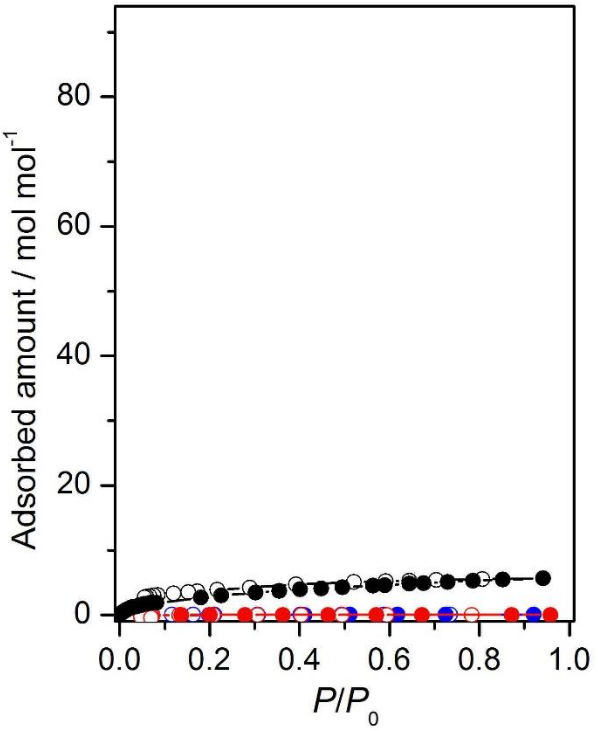

Fig. S17 Vapour adsorption (solid symbols) and desorption (open symbols) isotherms of **1** for H_2O (black), EtOH (blue), and acetone (red) vapours at 298 K.

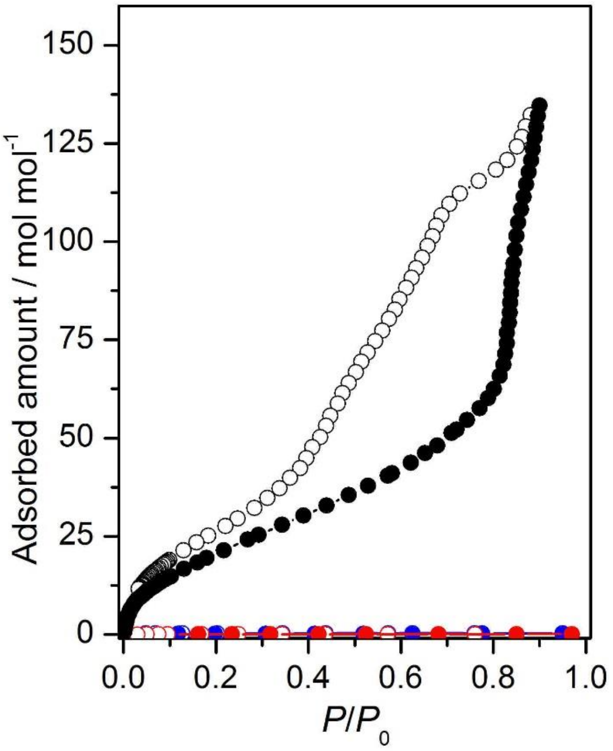

Fig. S18 Vapour adsorption (solid symbols) and desorption (open symbols) isotherms of **2** for H_2O (black), EtOH (blue), and acetone (red) vapours at 298 K.

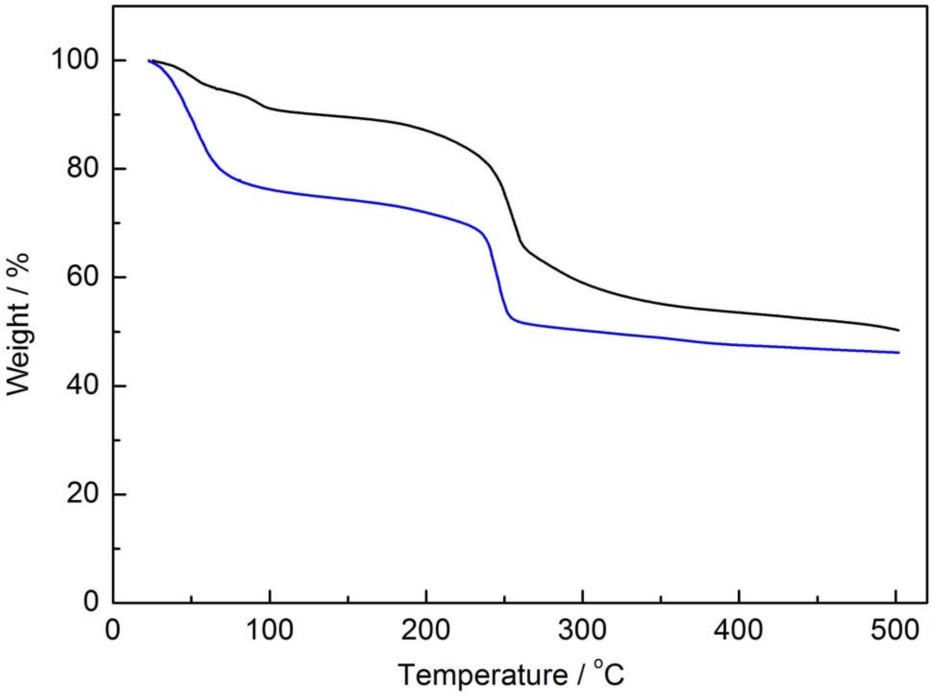

Fig. S19 Thermogravimetric curves for **1** (black) and **2** (blue).